

## 1. ICOSAHEDRAL TILINGS IN $\mathbb{R}^3$ : THE *ABCK* TILINGS.

Many real-world quasicrystals are based on icosahedral symmetry: Their diffraction images show five-fold, three-fold and two-fold symmetry, depending on the orientation of the probe. Two families of aperiodic tilings in  $\mathbb{R}^3$  with icosahedral symmetry are studied intensively in the literature. A member of the first family was found by R. Ammann, introduced by A.L. MacKay [13] and theoretically described by P. Kramer and R. Neri [10]. A member of the second family was found by J. Socolar and P. Steinhardt [18], and another member of this family by L. Danzer [6]. Each of the three tilings can be generated by local matching rules, as well as by cut-and-project methods. The two latter tilings can also be generated by inflation. The first family is obtained by a cut-and-project method from the primitive root lattice  $\mathbb{Z}^6$ , the second one from the root lattice  $D_6$ . Thus we refer to the first kind as *P*-type icosahedral tilings, and to the second kind as *F*-type, for ‘face-centred’, because of the correspondence of  $D_6$  to the face-centred cubic lattice  $D_3$ .

There is a third family of icosahedral tilings, generated by projection from  $D_6^*$ , the dual lattice of  $D_6$ . Because of the correspondence to the body-centred cubic lattice, these are called *B*-type tilings. This case is less prominent in the literature, thus we omit it. For a brief discussion of the three cases, see [3] or [2].

The *P*-type icosahedral tilings have two prototiles, one acute and one obtuse rhombohedron. Ten obtuse and ten acute prototiles can be assembled into a triacontahedron; this was noted already in 1935 by G. Kowalewski, compare [5]. An inflation for these prototiles was derived in [1]. For an illustrative description of the inflation, see [12]. Unfortunately, the inflation factor is pretty large, namely,  $\tau^3$ . This is one of the reasons that we will describe the *F*-type tilings in this section, rather than the *P*-type ones. The two *F*-type tilings by Socolar and Steinhardt and by Danzer are mld [15], [7]. Since there exists more literature on the Danzer tilings (the *ABCK* tilings), and since we consider them to have slightly simpler rules, they are discussed in the sequel.

**1.1. The inflation rule for *ABCK* tilings.** The *F*-type tilings found by Danzer use four tetrahedra *A, B, C, K* as prototiles, hence the name. These prototiles are derived as follows: Since one wants to construct tilings with icosahedral symmetry, one starts from the root system  $\Delta_{H_3}$ . Consider the family  $\mathfrak{F}$  of all tetrahedra whose faces are parallel to the mirror planes of the icosahedron. Thus all faces have normal vectors in  $\Delta_{H_3}$ . It turns out that there are exactly 15 similarity classes  $\mathcal{A}, \mathcal{B}, \dots, \mathcal{P}$  of such tetrahedra. All dihedral angles are multiples of  $\pi/2$ ,  $\pi/3$  or  $\pi/5$ . Moreover, each tetrahedron has at least one edge whose dihedral angle is a proper multiple of  $\pi/2$ ,  $\pi/3$  or  $\pi/5$ . By dividing such a dihedral angle into halves (resp. thirds), each tetrahedron is cut into two (resp. three) tetrahedra. The resulting tetrahedra

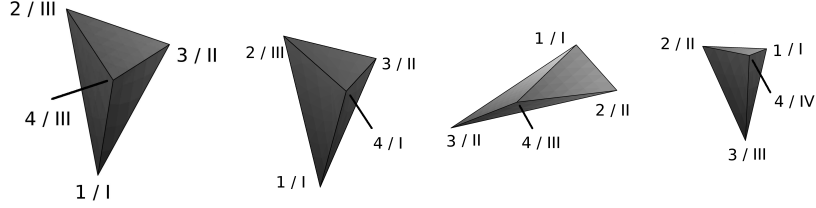


FIGURE 1. The prototiles  $A, B, C, K$  (from left to right). The Arabic numerals denote the number of each vertex, the Roman numerals the vertex classes, which arise from the CPS.

| prototile | vertex 1      | vertex 2                  | vertex 3                      | vertex 4                           |
|-----------|---------------|---------------------------|-------------------------------|------------------------------------|
| $A$       | $(0, 0, 0)$ I | $(\tau^3, 0, \tau^2)$ III | $(\tau^2, \tau^2, \tau^2)$ II | $(\tau^2, 1, 0)$ III               |
| $B$       | $(0, 0, 0)$ I | $(\tau^3, 0, \tau^2)$ III | $(\tau^2, \tau^2, \tau^2)$ II | $(\tau^2, \tau, 1)$ I              |
| $C$       | $(0, 0, 0)$ I | $(-\tau, 0, 1)$ II        | $(\tau^2, \tau^2, \tau^2)$ II | $(0, \tau^2, 1)$ III               |
| $K$       | $(0, 0, 0)$ I | $(-1, \tau, 0)$ II        | $(\tau, \tau, \tau)$ III      | $\frac{1}{2}(-1, 1/\tau, \tau)$ IV |

TABLE 1. The coordinates of the vertices of the prototiles, together with their vertex class (Roman numerals).

are still contained in  $\mathfrak{F}$ . In this way one obtains a tree of possible successors for each class of tetrahedra. For instance, a tetrahedron in  $\mathcal{A}$  might be dissected into two tetrahedra from  $\mathcal{L}$  and  $\mathcal{N}$ , or into two tetrahedra from  $\mathcal{B}$  and  $\mathcal{D}$ . By iterating these dissections, that is, by following the paths from each class, one can search for a small number  $k$  of classes such that each tetrahedron can be dissected into smaller tetrahedra contained in these  $k$  classes. It turns out that this is possible using just four classes  $\mathcal{A}, \mathcal{B}, \mathcal{C}$  and  $\mathcal{K}$ . For convenience, one desires a representative of each class whose coordinates are elements of  $\mathcal{M}_F$  (recall that  $\mathcal{M}_F$  is the  $\mathbb{Z}$ -span of  $2\Delta_{H_3}$ ). This can be achieved with only one exception. The coordinates of the vertices of the tetrahedra  $A, B, C, K$  are given in Table 1. Figure 1 depicts  $A, B, C$  and  $K$ , with the convention that the tetrahedra are sitting on their largest face and viewed from above. Note that the tetrahedron  $K$  has a vertex (number 4) whose coordinates are half integers with respect to  $\mathcal{M}_F$ . The three edges at this vertex are pairwise orthogonal.

The dissection of the tetrahedra  $A, B, C, K$  into similar tetrahedra has the further property that these similar tetrahedra are all congruent to  $\tau^{-1}A, \tau^{-1}B, \tau^{-1}C, \tau^{-1}K$ , respectively. This allows to define the inflation for the tiles  $A, B, C, K$ . Rather than listing the affine maps defining the inflation, which would be tedious and of questionable use, the inflation is depicted in Figure 2, see [14]

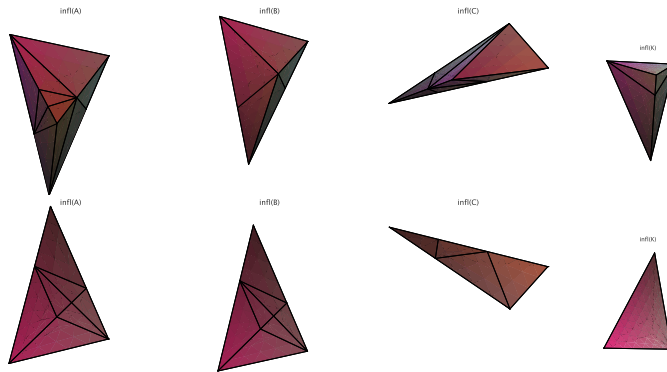


FIGURE 2. The inflation of the prototiles  $A, B, C, K$ . The inflated tiles are shown from ‘above’, as in Figure 1 (top row), and from ‘below’ (bottom row).

for an interactive online version. The inflation matrix is

$$M_{ABCK} = \begin{pmatrix} 0 & 0 & 1 & 0 \\ 3 & 2 & 0 & 1 \\ 2 & 1 & 2 & 0 \\ 6 & 4 & 2 & 1 \end{pmatrix}.$$

Its PF-eigenvalue is  $\lambda_{\text{PF}} = \tau^3$ , as it ought to be, since the inflation multiplier is  $\tau$ . The other eigenvalues are  $\tau$ ,  $-\tau^{-1}$ , and  $-\tau^{-3}$ . The normed PF-eigenvector, yielding the relative frequencies of the prototiles  $A, B, C, K$  in the inflation tiling, is

$$\begin{aligned} & \frac{1}{13\sqrt{5} + 30} (\sqrt{5}, 10 + 3\sqrt{5}, 5 + 2\sqrt{5}, 15 + 7\sqrt{5}) \\ & = (0.03785526\dots, 0.28285965\dots, 0.16035745\dots, 0.51892763\dots). \end{aligned}$$

Thus more than every second tile is of type  $K$ , and tiles of type  $A$  are quite rare. The tilings defined by these inflation are called  $ABCK$ -tilings in the sequel.

All the tetrahedra  $A, B, \dots, P$  (except  $K$ , which uses half-integer coordinates) can be realized with construction sets based on icosahedral symmetry, the most prominent probably being Zometool. There, the struts modelling edges are coloured red, yellow or blue, depending whether the strut is parallel to an axis of five-fold, three-fold or two-fold symmetry of the icosahedron. Therefore we adopt this colour scheme for the next section. Note that Danzer uses a different colour scheme in [6]. A comparison of the different colour schemes is shown in Table 2. Let us mention that many properties of the tetrahedra and their configurations in  $ABCK$  tilings are contained in the privately published book [8]. Unfortunately, this book contains several errors, some of which we correct here.

| parallel to | Zometool | Danzer |
|-------------|----------|--------|
| 5-fold      | red      | white  |
| 3-fold      | yellow   | green  |
| 2-fold      | blue     | red    |

TABLE 2. The edge colouring schemes of Zometool and Danzer.

**1.2. Local matching rules for  $ABCK$  tilings.** A local matching rule for the tiles  $A, B, C, K$  yielding  $ABCK$  tilings is particularly simple. First, all tiles are required to meet face-to-face. Second, if the face  $\Delta$  of a tetrahedron  $T$  contains an edge with dihedral angle  $\pi/2$  (a blue edge), then the mirror image of  $T$  has to be on the other side of  $\Delta$ . All tilings by prototiles  $A, B, C, K$  with these two properties are  $ABCK$  tilings.

The prototiles  $A, B$  and  $C$  have exactly one blue edge, where  $K$  has three of them, sharing one common vertex. As a consequence of the second rule, tiles of type  $A, B$  and  $C$  always come in quadruples around a blue edge, and tiles of type  $K$  come in groups of eight around a common vertex. The four, respectively eight, tiles together form an octahedra. Let us denote the octahedra obtained in this way by  $\langle A \rangle, \langle B \rangle, \langle C \rangle, \langle K \rangle$ , respectively. Note that  $\langle A \rangle$  and  $\langle B \rangle$  are not convex. The four octahedra may also be chosen as prototiles. We will refer to these new tilings by octahedra as  $\langle ABCK \rangle$  tilings. Since we can dissect each of the four octahedra into the corresponding tetrahedra uniquely (just dissect each octahedron along its mirror planes), the following lemma is immediate.

**Lemma 1.1.** *The  $ABCK$  tilings are mld to the  $\langle ABCK \rangle$  tilings.*  $\square$

The  $\langle ABCK \rangle$  tilings have two advantages: First, the half-integer vertex of  $K$  is not longer a vertex of the resulting tilings, and all vertices of this new tiling have integer coordinates with respect to  $\mathcal{M}_F$ . Second, the local matching rule becomes even simpler, since all blue edges vanish.

**Theorem 1.2.** *The  $\langle ABCK \rangle$  tilings can be obtained by a purely geometric local matching rule: All face-to-face tilings by tiles  $\langle A \rangle, \langle B \rangle, \langle C \rangle, \langle K \rangle$  are  $\langle ABCK \rangle$  tilings.*

Another realization of a local matching rule for the  $ABCK$  tilings uses Ammann planes. They are analogues of the Ammann bars for the Penrose tilings or Ammann-Beenker tilings. In [17] it is shown how to decorate the tiles  $A, B, C$  and  $K$  with plane sections, such that the local matching rule above can be replaced by the requirement that the tiles have to match face-to-face, and the planar sections within each tile extend to an infinite plane throughout the tiling.

The knowledge of the local matching rules simplifies the search for  $ABCK$  tilings which possess some global symmetry. It turns out that there are

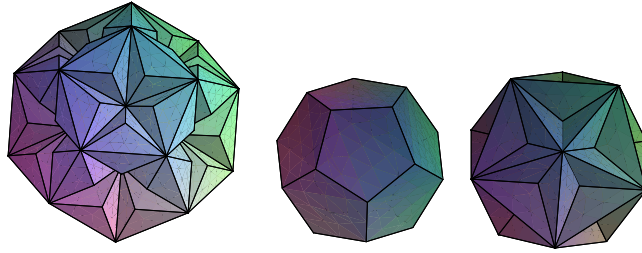


FIGURE 3. The windows for the vertex classes I, II and III of an  $ABCK$  tiling (from left to right). Vertex class IV, where eight tiles of type  $K$  touch each other, can not be obtained by projection in a consistent manner.

exactly three  $ABCK$  tilings with global icosahedral symmetry. They arise from the three local configurations with icosahedral symmetry. These are 120 copies of  $B$ , respectively  $C$ , respectively  $K$ , sharing a common vertex. With respect to Figure 1, it is vertex 1 of  $B$ , vertex 3 of  $C$ , and vertex 3 of  $K$ . Let us denote these vertex configurations by  $v_B, v_C, v_K$ . Under inflation these three are cyclically permuted: The inflation  $\sigma(v_B)$  contains  $v_C$  in its centre,  $\sigma(v_C)$  contains  $v_K$  in its centre, and  $\sigma(v_K)$  has  $v_B$  in its centre. Thus  $\sigma^3$  keeps each of them invariant. The infinite union  $\mathcal{T}_B := v_B \cup \sigma^3(v_B) \cup \sigma^6(v_B) \cup \dots$  is a well-defined tiling with global icosahedral symmetry. Analogously, the vertex configurations  $v_C$  and  $v_K$  yield tilings  $\mathcal{T}_C$  and  $\mathcal{T}_K$  with icosahedral symmetry. As with  $v_B, v_C, v_K$ , the tilings  $\mathcal{T}_B, \mathcal{T}_C, \mathcal{T}_K$  are cyclically permuted by  $\sigma$ . These are the only  $ABCK$  tilings with icosahedral symmetry, because there are no further local constellations with such symmetry. There are several more examples with lower global symmetry, arising in a similar way from vertex configurations with lower symmetry.

**1.3. CPS for the  $\langle ABCK \rangle$  tilings.** The  $ABCK$  tilings can be obtained by a CPS using the root lattice  $D_6$ . More precisely, the vertices of an  $ABCK$  tiling can be obtained by a CPS, except the vertices of class IV: As mentioned above, these vertices have half-integer coordinates in  $\mathcal{M}_F$ , thus they do not correspond to lattice points in  $D_6$ . This does not cause any problem, since the  $ABCK$  tilings are mld with the  $\langle ABCK \rangle$  tilings by Lemma 1.1. So in fact we describe the CPS for the vertices of the latter in the sequel. This was first carried out numerically by van Ophuysen, and in a rigorous manner in [9], [11].

The vertices of  $\langle ABCK \rangle$  tilings fall into the three distinct classes I, II, III mentioned above. Applying the Minkowski embedding [xxx referenz eintragen: Ex 3.8: Minkowski embedding of icosahedral modules] to the vertices of type I, II, III yields the following: vertices of type I are mapped to vertices of  $D_6$ , whereas vertices of type II are mapped to  $D_6 + (-1, \tau, 0, -\tau, -1, 0)$ ,

and vertices of type III are mapped to  $D_6 + (\tau, \tau, \tau, -1, -1, -1)$ . Thus each vertex type arises from some coset of  $D_6$ . A more natural description is given in the sequel.

Remark: as in Ex 3.8, 3.9 [xxx referenz eintragen], the Minkowski embedding yields a scaled copy of the standard root lattice  $D_6$ . Here we work with this scaled copy of  $D_6$ , rather than the standard root lattice  $D_6$ . We will call this scaled lattice also  $D_6$ . By choosing an appropriate bilinear form this yields the standard root lattice  $D_6$ .

The root lattice  $D_6$  possesses three classes of *holes*. Holes are points whose distance to  $D_6$  is a local maximum [4]. Those holes whose distance to  $D_6$  is a global maximum are called *deep holes*, the other holes are called *shallow holes*. The lattice  $D_6$  possesses one class of deep holes: the coset  $D_6 + (\tau, 0, 1, -1, 0, \tau)$ , and two classes of shallow holes: the cosets  $D_6 + (\tau, 0, 0, -1, 0, 0)$  and  $D_6 + (1, 0, 0, -\tau, 0, 0)$ . Note that in this setup we can immediately decide to which one of the four cosets a given vector belongs to: Consider the first three entries. If both the number of  $\tau$ s and the number of 1s are even, the vector of the first three entries is an element of  $\mathcal{M}_F$ . By the Minkowski embedding construction of  $D_6$ , the entire vector is an element of  $D_6$ . If both the number of  $\tau$ s and the number of 1s are odd, it is a deep hole, etc.

Keeping this fact in mind, the three vertex classes of the  $\langle ABCK \rangle$  tilings arise from the three classes of holes: Vertices of class III are projections of the deep holes, where the projection is just the orthogonal projection from  $\mathbb{R}^6$  to  $\mathbb{R}^3$  by omitting the last three entries. Vertices of class II are projections of the shallow holes  $D_6 + (\tau, 0, 0, -1, 0, 0)$ , and vertices of class I are projections from the shallow holes  $D_6 + (1, 0, 0, -\tau, 0, 0)$ . The vertices of  $D_6$  itself don't correspond to any vertex in the tilings. In order to make the coordinates of Table [xxx Referenz eintragen: Table 6.1, Koordinaten der ABCK tiles] compatible with this setup, shift each vertex in the table by  $(1, 0, 0)$ . Then one can check for instance: Vertex 1 of tile  $A$  (type I) is  $(1, 0, 0)$ , corresponding to  $(1, 0, 0, -\tau, 0, 0)$ , a shallow hole (of the second kind). Vertex 2 of tile  $A$  is  $(2\tau + 1, 0, \tau + 1)$ , corresponding to  $(2\tau + 1, 0, \tau + 1, -2 + \tau, 0, -1 + \tau)$ . In the first three entries, we count three  $\tau$ s (odd) and two 1s (even), thus this vertex is projected from a shallow hole in  $D_6 + (\tau, 0, 0, -1, 0, 0)$ . In a similar way, one can check explicitly how moving from a vertex of type I to a vertex of type II corresponds to moving from one coset to another.

In the Penrose tilings, the vertices occur in four distinct classes, and the CPS for the Penrose tilings uses the internal space  $\mathbb{R}^2 \times C_5$ . The  $C_5$ -coordinate enumerates the four classes of vertices. More precisely, it enumerates the five vertex classes, where one class is empty. Analogously, we can formulate the CPS for the  $\langle ABCK \rangle$  tilings using the internal space  $\mathbb{R}^3 \times C_4$ , where the  $C_4$ -coordinate enumerates the vertex classes of the  $\langle ABCK \rangle$  tilings, with

one class being empty. Then, the appropriate lattice in  $\mathbb{R}^6 \times C_4$  would be  $D_6 \times C_3$ .

Alternatively, one might formulate three different CPS, one for each vertex class, each of them using the same setup, but three different windows. For simplicity, we will describe the latter alternative now, relying heavily on [11].

For each single vertex class, the lattice is  $D_6$ , in the form described above. Then projection to direct space is omitting the last three entries from each lattice point, and projection to the internal space is omitting the first three entries. The symmetry group of  $D_6$  contains an icosahedral group  $I$ . The two 3D subspaces to which we project are both fixed under the action of  $I$ . The windows of the three distinct vertex classes are shown in Figure 3, see also [14] for an interactive online version. The window for vertex class II is a regular dodecahedron of edge length 2. (Compare [11]: there the authors obtain a dodecahedron of edge length  $e := (2/(\tau + 2))^{1/2}$ . Our  $D_6$  is scaled by  $\sqrt{2}\sqrt{\tau + 2} = \sqrt{24}\cos(\pi/10)$  w.r.t. their lattice.) The window for vertex class III is a so called great dodecahedron, one of the Kepler-Poinsot polyhedra, or regular star polyhedra. Its long edges have length  $2\tau$ . The window for vertex class I is also a polyhedron with icosahedral symmetry, but we are not aware of any name of it. It can be seen as a regular dodecahedron with five-fold stars engraved on each pentagonal face. Its long edges have length  $4\tau/\sqrt{\tau + 2}$ . The volumes of the windows yield the frequencies of the vertices of class I, II, III in any  $\langle ABCK \rangle$  tiling. The volume of window I is  $20(5\tau + 2)$ . The volume of window II is  $4(7\tau + 4)$ , and the volume of window III is  $20\tau^2$ . If we denote the average number of points of class  $x$  per unit volume by  $d_x$ , then we obtain by the density formula  $d_x = \text{vol}(\text{window } x) / \det(D_6) = \text{vol}(\text{window } x) / (16(\tau + 2)^3)$ . The numerical values are

$$d_{\text{I}} = 0.26631\dots, \quad d_{\text{II}} = \frac{\tau}{20} = 0.0809016994\dots, \quad d_{\text{III}} = 0.069098300\dots$$

Thus the density of the vertices in  $\langle ABCK \rangle$  tilings is  $d_{\text{I}} + d_{\text{II}} + d_{\text{III}} = (37\tau + 19) / (20(4\tau + 3)) = 0.416311896\dots$

**Theorem 1.3.** *Each of the vertex classes I, II, III of the  $\langle ABCK \rangle$  tilings are model sets, with internal space  $\mathbb{R}^3$  and lattice  $D_6$ . The union of the three vertex classes is a model set with internal space  $\mathbb{R}^3 \times C_4$ .*

The windows were determined numerically by van Ophuyssen, and constructively in [11]. The model set property of  $\langle ABCK \rangle$  is proved in [11] by showing that the  $\langle ABCK \rangle$  are locally derivable from a further  $F$ -type projection tiling, called  $\mathcal{T}^{(2F)}$ .

The fact that the  $\langle ABCK \rangle$  tilings can be generated by a CPS, together with the fact that  $\langle ABCK \rangle$  tilings and  $ABCK$  tilings are mld yield the following result.

**Theorem 1.4.** *Both the  $\langle ABCK \rangle$  and the  $ABCK$  tilings are pure point diffractive.*

**1.4. Relations to other icosahedral tilings.** As mentioned above, the  $ABCK$  tilings are mld with the Socolar-Steinhardt tilings [15], [7]. The latter ones use four zonohedra as prototiles: a rhombic hexahedron, a rhombic dodecahedron, a rhombic icosahedron and a rhombic triacontahedron. It turns out that the vertices of the Socolar-Steinhardt tilings are exactly the vertices of classes II and III in the  $ABCK$  tilings. Thus the above discussion yields immediately a CPS for the Socolar-Steinhardt tilings. A local matching rule for these tilings is achieved by decorating the rhombic facets with three distinct markings, and requiring that faces have to match with respect to these markings. The Socolar-Steinhardt tilings possess also an inflation with factor  $\tau$ , but not a stone inflation. For a detailed discussion of the Socolar-Steinhardt tilings, see [18].

There is a further  $F$ -type tiling, called  $\mathcal{T}^{(2F)}$ , obtained by projection. The  $ABCK$  tilings are locally derivable from  $\mathcal{T}^{(2F)}$ , but not vice versa [11].

#### REFERENCES

- [1] M. Audier, P. Guyot: A perfect icosahedral atomic structure: A two-unit-cell and four-zonohedra description, *Phil. Mag. Lett.* 58 (1988) 17-23.
- [2] M. Baake: A guide to mathematical quasicrystals, in: *Quasicrystals*, eds J.-B. Suck, M. Schreiber, P. Häußler, Springer, Berlin 2004.
- [3] M. Baake, D. Joseph, P. Kramer, M. Schlottmann: Root lattices and quasicrystals, *J. Phys. A: Math. Gen.* 23 (1990) L1037-L1041.
- [4] J.H. Conway, N.J.A. Sloane: *Sphere packings, Lattices and Groups*, 2nd ed, Springer (1993).
- [5] H.S.M. Coxeter: *Regular Polytopes*, 3rd edition, Dover, New York (1973).
- [6] L. Danzer: Three-dimensional analogs of the planar Penrose tilings and quasicrystals, *Discrete Math.* 76 (1989) 1-7.
- [7] L. Danzer, Z. Papadopolos, A. Talis: Full equivalence between Socolar's tilings and the  $(A, B, C, K)$ -tilings leading to a rather natural decoration, *Int. J. Mod. Phys. B* 7 (1993) 1379-1386.
- [8] L. Danzer, P. Sonneborn, G. van Ophuysen, S. Duitmann: The  $\{A,B,C,K\}$ -Book, Univ. Dortmund (1993).
- [9] G. Kasner, H. Böttger: Lattice dynamics of an F-type icosahedral quasicrystal, *Int. J. Mod. Phys. B* 7 (1993) 1487-1504.
- [10] P. Kramer, R. Neri: On periodic and nonperiodic space fillings of  $E^m$  obtained by projection, *Acta Cryst. Sect. A* 40 (1984) 580-587, Erratum: *Acta Cryst. Sect. A* 41 (1985) 619.
- [11] P. Kramer, Z. Papadopolos, M. Schlottmann, D. Zeidler: Projection of the Danzer tiling *J. Phys. A: Math. Gen.* 27 (1994) 4505-4517.
- [12] E.A. Lord, S. Ranganathan, U.D. Kulkarni: Tilings, coverings, clusters and quasicrystals, *Current Sci.* 78 (2000) 64-72.
- [13] A.L. Mackay: De nive quinquangula: on the pentagonal snowflake (Russian) *Soviet Phys. Cryst.* 26 (1981) 910-919; reprinted in [16].
- [14] D. Frettlöh, E. Harriss: Tilings Encyclopedia, [xxx Spaeter aendern:] [www.math.uni-bielefeld.de/baake/frettlloe/abck/inflabck.html](http://www.math.uni-bielefeld.de/baake/frettlloe/abck/inflabck.html)  
[www.math.uni-bielefeld.de/baake/frettlloe/abck/winabck.html](http://www.math.uni-bielefeld.de/baake/frettlloe/abck/winabck.html)

- [15] J. Roth: The equivalence of two face-centred icosahedral tilings with respect to local derivability, *J. Phys. A* 26 (1993) 1455-1461.
- [16] P.J. Steinhardt, S. Ostlund (eds.): *The physics of quasicrystals*, World Scientific Publishing Co., Singapore (1987).
- [17] T. Stehling: Ammann bars and quasicrystals, *Discrete Comput. Geom.* 7 (1992) 125-133.
- [18] J.E.S. Socolar, P.J. Steinhardt: Quasicrystals II: Unit cell configurations, *Phys. Rev. B* 34 (1986) 617-647.